

High Uranium Extraction by Polydopamine Functionalized MXene from Aqueous Solutions

Pengcheng Gu^{1,*}, Dichen Xia¹, Yan Liu¹, Quan Chen¹, and Lingling Wang^{2,3}

¹School of Resources and Environment, Anhui Agricultural University, Hefei 230036, China

²School of Earth and Space Sciences, University of Science and Technology of China, Hefei, China

³Anhui Academy of Environmental Science Research, Hefei, China

Abstract. MXenes were outstanding materials for aqueous environment remediation, MXenes with a high capacity for radionuclides uranium (U(VI)) remains a challenge. In this study, a novel polydopamine functionalized MXene (defined as MXene@PDA) was successfully synthesised and evaluated for the aggregation towards U(VI) from wastewater. Versatile PDA owing functional groups provided more sites to capture contaminant ions. The mechanism research with MXene@PDA was explored by batch experiments together with the XPS analyses. The results revealed MXene@PDA with abundant functional groups exhibited superior elimination ability (90.4 mg/g) at pH = 5.0. The mechanism of U(VI) on MXene@PDA was primarily ascribed to the surface complexation force between the UO_2^{2+} and -OH, NH_2 groups. The PDA modification of MXene materials are proved to be excellent materials for the extraction of radionuclides in the aqueous solution.

1 Introduction

With the depletion of resources, nuclear power has been deemed as a key resource in energy system and become an alternative to the traditional energy[1,2]. However, various radioactive contaminants, such as ^{235}U and ^{154}Eu poses a fatal threat to environmental protection and human health. As the main fuel for current commercial reactors, uranium with high internal radiation and long half-life, and even at very low concentrations can cause damage to the environment and organisms[3].

To date, various two-dimensional materials have been widely used in the dispose of radioactive wastewater. Layered double hydroxides (LDHs), metal organic frameworks (MOFs). Unfortunately, most of the above materials inevitably endure slow adsorption speed, limited adsorption capacities and poor selectivity, making them unsuitable for practical applications[4,5].

Recently, an emerging class of two-dimensional transition metal carbide (MXene), has emerged in the environmental fields because of the unique physical and chemical properties. In particular, multilayered MXenes are promising candidates for clean-up of several radionuclide cations (^{238}U and $^{107}\text{Pd}^{2+}$) through the coordination interaction, ion exchange and reduction immobilization[6]. For example, Wang et al reported V_2CT_x showed the remarkable removal capacity towards U(VI)[7]. Additionally, another $\text{Ti}_3\text{C}_2\text{T}_x$ with more efficient adsorption properties for U(VI) was further reported by Wang's groups. Furthermore, the interaction mechanism of adsorption-reduction in the elimination process of U(VI) was revealed[8]. It can't be ignored that

the absence of abundant functional groups greatly hinder its inherent sewage purification capacity. To address this problem, various investigations have been devoted to the design of functionalized MXene material for enhancing its removal performances. All in all, limitations of U(VI) include low removal capacity and poor selectivity, and novel functionalized MXene materials with high sequestration capacity for U(VI) remain a goal.

Polydopamine (PDA), an excellent biopolymer, has attracted multidisciplinary interests benefit from its outstanding biocompatibility, strong adhesive force and abundant functional groups[9,10]. The PDA layer can be easily decorated on the surface of various substrates by spontaneous polymerization of dopamine. Because of these advantages, as an important coating material PDA provided an excellent platform for binding metals through covalent and non-covalent interactions including hydrogen bonds, electrostatic interactions etc. In the past decade, several researchers devote lots of energy to utilize PDA for surface modification of several materials. As expected, the PDA-coated nanocomposites exhibited the outstanding performance to several pollutant ions. Hence, the PDA with the versatile merits could be considered as potential material to capturing U(VI) from aqueous solution.

Herein, a novel polydopamine functionalized $\text{Ti}_3\text{C}_2\text{T}_x$ (defined as $\text{Ti}_3\text{C}_2\text{T}_x @\text{PDA}$) was synthesised and evaluated for the uptake of U(VI) from wastewater. The interaction mechanism was further researched by batch experiments and XPS analyses. The batch experiments revealed that MXene@PDA with abundant functional groups exhibited superior removal capacity (90.4 mg/g)

*Corresponding author: gupc518@163.com

at $T = 293\text{K}$ and $\text{pH} = 5.0$. Furthermore, the XPS analyses exhibited that the interaction mechanism of U(VI) on the $\text{Ti}_3\text{C}_2\text{T}_x @\text{PDA}$ was primarily ascribed to the complexation force between UO_2^{2+} and rich functional groups (hydroxyl and amine groups). PDA functionalized MXene composites are proved to be excellent materials for the extraction of radioactive nuclear wastewater.

2 Materials and Operation Methods

2.1 Preparation of $\text{Ti}_3\text{C}_2\text{T}_x @\text{PDA}$

Typically, 100 mg Ti_3AlC_2 powders (purchased from Forsman Technology Company) was added to 21 mL of solution including 1 M LiF and 6 M HCl group by group. And then, after magnetic stirring for 48 h at 45°C for 48h, the obtained outcome was centrifuged for 30 min at 3500 rpm and washed 8 times. The supernatant is collected with water until the pH drops to 6, it was dried in oven at 80°C for ~12 hours. The final product was $\text{Ti}_3\text{C}_2\text{T}_x$. And then, 220 mg $\text{Ti}_3\text{C}_2\text{T}_x$ was dissolved in 120 mL Tris buffer, followed by ultrasonic treatment for 15 min, adding 220 mg dopamine, and mechanical agitation for overnight. The obtained residues was washed six times using ultrapure water and ethanol and desiccated for ~12 h in an oven at 80°C . The grey powder was named as $\text{Ti}_3\text{C}_2\text{T}_x @\text{PDA}$.

2.2 Batch Adsorption

Firstly, a certain amount of $\text{UO}_2(\text{NO}_3)_2 \cdot 6\text{H}_2\text{O}$ was dissolved in deionized water, the origin solution of U(VI) was prepared (200 mg L^{-1}). Various concentrations of U(VI) were carried out on $\text{Ti}_3\text{C}_2\text{T}_x$ at 25°C . Adsorption isotherm studies explored adsorption experiments at $\text{pH} = 5.0$ and a series of concentrations. The adsorption rate (%) and adsorbability (Q_e) are counted by the formula below [11]:

$$q_e = \frac{V \times (C_0 - C_e)}{m} \quad (1)$$

$$\text{Adsorption}\% = \frac{(C_0 - C_e)}{C_0} \times 100 \quad (2)$$

Here, C_0 ($\text{mg} \cdot \text{L}^{-1}$) is the original concentration, C_e ($\text{mg} \cdot \text{L}^{-1}$) is the equilibrium concentration, m (mg) and V (mL) represent the dosage of $\text{MXene} @\text{PDA}$ together with the total volume of the suspension.

2.3 Instrumentation

In this study, the morphologies of MXene samples was determined by S-4800 (SEM). The X-ray diffraction (XRD) patterns was characterized by A Bruker D8 advance diffractometer (over a sweep speed of 10/min at the region from 5°C to 80°C). The XPS dates was equipped with the Al X-ray source, which operated at 10 kV. with an Al $K\alpha$ source at 1486.8 eV.

3 Results & Discussion

3.1 Characterization

The structures of original MXene ($\text{Ti}_3\text{C}_2\text{T}_x$) together with $\text{MXene} @\text{PDA}$ was characterized in virtue of SEM. As shown in Fig. 1A, The Al layers were removed and a representative exfoliated morphology of layered $\text{Ti}_3\text{C}_2\text{T}_x$ (layered organ-like) was successfully obtained.

After modification with dopamine, Fig. 1B clearly shows irregular outer edges and thickened edges of $\text{Ti}_3\text{C}_2\text{T}_x$, which distinctly indicates that the shuck of PDA is evenly wrapped in $\text{Ti}_3\text{C}_2\text{T}_x$. The morphologic evolution of the original organ-like $\text{Ti}_3\text{C}_2\text{T}_x$ confirms the successful surface modification of PDA.

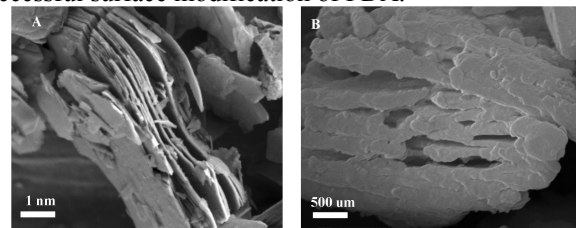


Fig. 1. (A) SEM images of $\text{Ti}_3\text{C}_2\text{T}_x$; (B) SEM images of $\text{Ti}_3\text{C}_2\text{T}_x @\text{PDA}$.

The crystal structure transformation of samples were further measured by XRD. As presented in Fig. 2A, The as-synthesized $\text{Ti}_3\text{C}_2\text{T}_x$ shows a featured (002), (004) peaks at 7.84° and 15.6° , which were consistent with those obtained by predecessors [12]. The intensity of the typical peak representing $\text{Ti}_3\text{C}_2\text{T}_x$ was significantly reduced and flattened after dopamine modified. The XPS spectra in Fig. 2b revealed that Ti, O and C are the mainly constituents on the surface of $\text{Ti}_3\text{C}_2\text{T}_x$. Obviously, an appearance of distinct N 1s sharp peak was captured from the $\text{Ti}_3\text{C}_2\text{T}_x @\text{PDA}$ samples compared with the pristine $\text{Ti}_3\text{C}_2\text{T}_x$, demonstrating that the successful surface modification PDA[9].

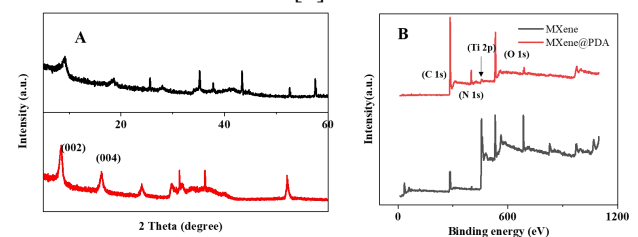


Fig. 2. (A) XRD patterns of $\text{Ti}_3\text{C}_2\text{T}_x$ and $\text{Ti}_3\text{C}_2\text{T}_x @\text{PDA}$; (B) XPS spectra of $\text{Ti}_3\text{C}_2\text{T}_x$ and $\text{Ti}_3\text{C}_2\text{T}_x @\text{PDA}$.

3.2 Thermodynamic studies

The results of U(VI) uptake by $\text{Ti}_3\text{C}_2\text{T}_x @\text{PDA}$ are presented in Fig. 3. Fig. 3A shows a U(VI) adsorption isotherms for $\text{Ti}_3\text{C}_2\text{T}_x @\text{PDA}$ under different temperatures ($298 \text{ K} - 328 \text{ K}$). Obviously, with the temperature increasing, the maximum value (Q_e) intends to rise, manifesting that the higher temperature will accelerate the elimination of U(VI) . Furthermore, the following models are used to simulate the isotherms results, refers as[13]:

Langmuir model:

$$q_e = \frac{K_L Q_{e,max} C_e}{1 + K_L C_e} \quad (3)$$

Freundlich model:

$$Q_e = K_f C_e^{\frac{1}{n}} \quad (4)$$

Q_e represents the mass of U(VI), which is adsorbed on the $Ti_3C_2T_x@PDA$, C_e means the equilibrium concentration, Q_{max} signifies the saturated elimination performance, and B ($L \cdot mol^{-1}$) represents the constant correlated to the heat of adsorption. K_f is the elimination ability, which the equilibrium concentration was close to 1; the n represents the adsorption dependence degree.

The relevant fitting parameters are shown in Table 1. Comparison to the regression coefficients (R^2), the immobilization isotherms was more in line with the Langmuir model. Furthermore, the maximum fixation ability of $Ti_3C_2T_x@PDA$ theoretically derived to be 90.4 mg/g at 313 K. This obtained results suggest the excellent adsorption capacity may be caused by the abundant oxygen-containing function group and amine functionalization, which synergistically accelerated the uptake of U(VI).

Table 1. The fitted parameters calculated by two models

Parameters	$K_L(L/mg)$	$Q_{e,max}(mg/g)$	R^2
Langmuir	0.95	90.4	0.93
Freundlich	0.93	-	0.87

To study the thermodynamic feasibility and intrinsic characteristics of adsorption process, the thermodynamic parameters (ΔG^0 , ΔH^0 and ΔS^0) are calculated from the adsorption isotherms varying with temperature. The positive ΔH^0 values of 9.78 kJ mol^{-1} for $Ti_3C_2T_x@PDA$ indicated that the feature endothermic of adsorption process. Meanwhile, the positive ΔS^0 value further affirms the traits of high affinity of U(VI) for $Ti_3C_2T_x@PDA$. Additionally, The value of ΔG^0 is negative, further also indicating the adsorption process was spontaneous. All in all, the thermodynamic parameters reflect that $Ti_3C_2T_x@PDA$ exhibit outstanding adsorption potential for U(VI) in aqueous solution.

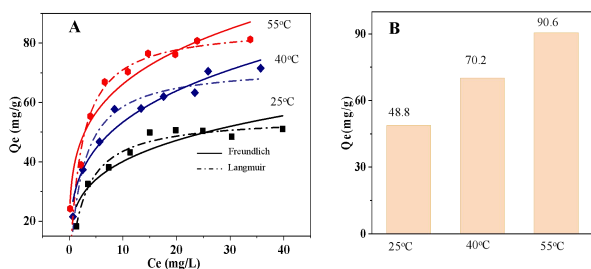


Fig. 3. (A)Uranium adsorption isotherms for $Ti_3C_2T_x@PDA$; (B)Diagram of removal capacity of U(VI) on $Ti_3C_2T_x@PDA$ at different temperatures.

3.3. Effect of pH

In general, the pH plays a leading part in the migration of pollutant, especially in the aqueous solution. Therefore, the adsorption mechanism is explored through exploring the influence of pH and ionic strength[14]. As presented by Figure 4, the solution pH presents a evident impact on the adsorption of $Ti_3C_2T_x@PDA$ on U(VI), which was divided into two regions. The uptake ability of $Ti_3C_2T_x@PDA$ increases with the pH increasing from 1.5 to 6.5 by degrees. Subsequently, the adsorption percentage declined at $6.5 < pH < 11.0$. According to previous studies, the point of zero charge (pH_{PZC}) of $Ti_3C_2T_x@PDA$ were approximately 4.0, noting the surface of $Ti_3C_2T_x@PDA$ is negatively charged over a wide pH range[8]. when pH lower to the pH_{PZC} , the fierce electrostatic repulsion together with competition towards H^+ are the primarily limiting factors for the uptake of U(VI). Under this pH condition U(VI) is mainly in the form of positive charge $UO_2(OH)^{2+}$, $UO_2(OH)^+$ and UO_2^{2+} [15]. As pH increasing from pH_{PZC} to 6.5, the formation precipitation (UO_2CO_3) is the main removal mechanism. As result, the removal rate is significantly improved. However, accompanied by the increase of pH, the uptake percentage was significant reduction. In the range of 6.5-11.0, the forming species of $UO_3(CO_3)_3^{4-}$ and $UO_3(CO_3)_2^{2-}$ were difficult to be adsorbed on $Ti_3C_2T_x@PDA$, which was negatively charged. The above mentions were the main reason for the reduced removal rate.

The ionic strength of U(VI) adsorption on $Ti_3C_2T_x@PDA$ was performed in different concentrations $NaNO_3$ solutions (0.001M, 0.01M and 0.1M), respectively (Fig. 4). The extraction of U(VI) on $Ti_3C_2T_x@PDA$ is significantly correlated with the ionic strength. In the whole pH range, it was found that the lower the salt concentration, the stronger the absorption efficiency of U(VI). This phenomenon revealed that the elimination process may be dominated by surface complexation.

With the decrease of ionic strength, the competition between Na^+ and U(VI) weakens, and the effective sites of U(VI) was increased[16]. It can be explained as follows: one hand, the increase of ionic strength presents a negative effect on the activity coefficient of U(VI), limiting the movement of U(VI) from solution to surface. On the other hand, the solid particles tend to accumulate in high ionic concentrations, which greatly reduces the available combining sites for ion exchange and thus reduces the elimination of U(VI) on the $Ti_3C_2T_x@PDA$. Finally, the increase of the thickness of the electric double layer inhibits the electrostatic attraction, thus further reducing the uptake of U(VI) by $Ti_3C_2T_x@PDA$ at high salt concentration. Base on the above discussion, the interaction mechanism can be described by surface complexation of the outer sphere[17].

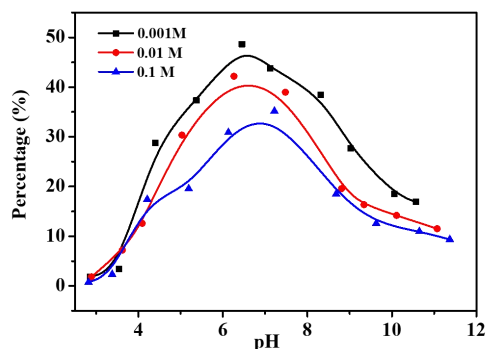


Fig. 4. Effect of pH and ionic strength on the uranium extraction efficiency

3.4. Mechanism Investigation

The interaction mechanism was further confirmed by XPS technique. The samples before ($Ti_3C_2T_x@PDA$) and after extraction ($Ti_3C_2T_x@PDA-U(VI)$) were presented in the Fig. 5 and Table 2. It could be seen in Fig. 5(A) that the O 1s of $Ti_3C_2T_x@PDA$ spectrum was divided into three component peaks located at 532.8, 531.2, and 533.3 eV, which were ascribed to the groups C=O, C-O and O-H[10]. Compared to pristine $Ti_3C_2T_x@PDA$, the peak position of C-O and -OH were shifted to 532.3 eV and 533.0 eV, respectively. The shifted of position indicated that a new bond was formed between O and U(VI)[14,17]. Furthermore, the quantity of -OH increased from 40.4% to 29.5% after adsorption. The change of peaks position and quantity showed that the oxygen-containing functional groups (such as -OH) plays an key part in the adsorption process. For the N 1s spectrum (Figure 5B and Table 2), the N 1s spectrum of $Ti_3C_2T_x@PDA$ located at 400.0 eV and 402.5 eV, which were ascribed to the groups -N= and the -NH₂. The -NH₂ group is present because of the introduction of PDA layer. It is clear that no discernible difference was observed for -N = species (400.00 eV). However, the peak of -NH₂ (402.5 eV) changed to a lower binding energy (401.5 eV)[9]. This phenomenon indicates that the -NH₂ functional group may combine with U(VI), which is one of the fundamental reasons for the efficient extraction of U(VI). Therefore, benefited from hydroxyl groups and amine groups from PDA, the interaction mechanism between $Ti_3C_2T_x@PDA$ and U(VI) was majorly ascribed to the surface complexation .

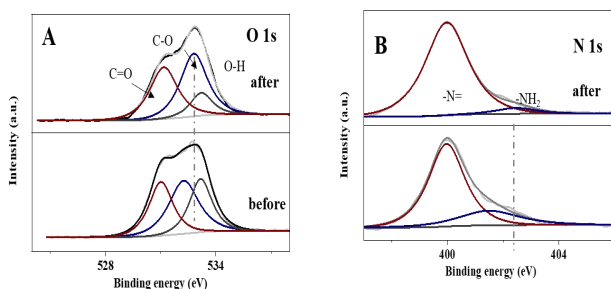


Fig. 5. XPS spectra of $Ti_3C_2T_x@PDA$ of U(VI) uptake. (A,B) high-resolution O 1s and N 1s region.

Table 2. Binding energies of $Ti_3C_2T_x@PDA$: O and N before and after U(VI) adsorption.

Peaks	E_B (eV)	O 1s (eV)			N 1s (eV)	
		C-O	-OH	C=O	-N=	-NH ₂
$Ti_3C_2T_x@PDA$		532.8	533.3	531.2	400.0	402.5
$Ti_3C_2T_x@PDA-U$		532.3	533.0	531.2	400.0	401.5

4 Conclusion

As consequence, this work reported a novel polydopamine functionalized $Ti_3C_2T_x$ (defined as $Ti_3C_2T_x @PDA$) and applied as U(VI) scavenger from. Owing abundant functional groups, The PDA could provide multifarious sites to fix contaminant ions. Based on the XPS analyses O 1s and N 1s, the excellent affinity of MXene@PDA towards U(VI) could be mainly ascribed to their coordination interaction with hydroxy groups and amine functional groups. The batch experiments revealed that MXene @PDA with abundant functional groups exhibited superior elimination performance (90.4 mg/g) . This work provides guidance for the development of MXene adsorbents with excellent uranium extraction ability .

Acknowledgements

This work was supported by the Natural Science Foundation of Anhui Province (NO. 2008085QB59), the National Natural Science Foundation of China (NO. 22006002) and Key research project of Ecological environment in Anhui Province HKYKY05 -2021.

References

1. P. Zhang, L. Wang, K. Du, S. Wang, Z. Huang, L. Yuan, Z. Li, H Wang, L. Zheng, Z. Chai and W. Shi Effective removal of U(VI) and Eu(III) by carboxyl functionalized MXene nanosheets. *J. Hazard. Mater.*, **396**, 122731-122739 (2020)
2. S. Huang, S. Jiang, H. Pang, T. Wen, A.M. Asiri, K.A. Alamry, A. Alsaedi, X. Wang and S. Wang, Dual functional nanocomposites of magnetic MnFe₂O₄ and fluorescent carbon dots for efficient U(VI) removal. *Chem. Eng.*, **368**, 941-950 (2019)
3. P. Gu, S. Zhang, C. Zhang, X. Wang, A. Khan, T. Wen, B. Hu, A. Alsaedi, T. Hayat and X. Wang, Two-dimensional MAX-derived titanate nanostructures for efficient removal of Pb(II). *Dalton Trans.*, **48**, 2100-2107 (2019)
4. G. Cheng, A. Zhang, Z. Zhao, Z. Chai, B. Hu, B. Han, Y. Ai and X. Wang, Extremely stable amidoxime functionalized covalent organic frameworks for uranium extraction from seawater with high efficiency and selectivity. *Sci. Bull.*, **66(19)**, 1994-2001 (2021)
5. C.L. Xiao, Z.H. Fard, D. Sarma, T.B. Song, C. Xu and M.G. Kanatzidis, Highly Efficient Separation

- of Trivalent Minor Actinides by a Layered Metal Sulfide (KInSn₂S₆) from Acidic Radioactive Waste. *J. Am. Chem. Soc.*, **139**,16494-16497 (2017)
6. W. Mu, S. Du, X. Li, Q. Yu, H. Wei, Y. Yang and S. Peng, Removal of radioactive palladium based on novel 2D titanium carbides. *Chem. Eng. J.*, **358**, 283-290 (2019)
 7. L. Wang, L. Yuan, K. Chen, Y. Zhang, Q. Deng, S. Du, Q. Huang, L. Zheng, J. Zhang, Z. Chai, M.W. Barsoum, X. Wang and W. Shi, Loading Actinides in Multilayered Structures for Nuclear Waste Treatment: The First Case Study of Uranium Capture with Vanadium Carbide MXene. *ACS Appl. Mater. Interfaces.*, **8**, 16396-16403 (2016)
 8. L. Wang, H. Song, L. Yuan, Z. Li, P. Zhang, J.K. Gibson, L. Zheng, H. Wang, Z. Chai and W. Shi, Effective Removal of Anionic Re(VII) by Surface-Modified Ti₂CT_x MXene Nanocomposites: Implications for Tc(VII) Sequestration. *Environ. Sci. Technol.*, **53**, 3739-3747 (2019)
 9. D. Yang, X. Wang, N. Wang, G. Zhao, G. Song, D. Chen, Y. Liang, T. Wen, H. Wang and T. Hayat, In-situ growth of hierarchical layered double hydroxide on polydopamine-encapsulated hollow Fe₃O₄ microspheres for efficient removal and recovery of U(VI). *J. Clean. Prod.*, **172**, 2033-2044 (2017)
 10. X. Wang, N. Wang, D. Yang, X. Wang, S. Yu, H. Wang, T. Wen, G. Song and Z. Yu, Highly efficient Pb(II) and Cu(II) removal using hollow Fe₃O₄@PDA nanoparticles with excellent application capability and reusability[J]. *Inorg. Chem. Front.*, **5**, 2174-2182 (2018)
 11. L. Yin, Y. Hu, R. Ma, T. Wen, X. Wang, B. Hu, Z. Yu, T. Hayat, A. Alsaedi and X. Wang, Smart construction of mesoporous carbon templated hierarchical Mg-Al and Ni-Al layered double hydroxides for remarkably enhanced U(VI) management. *Chem. Eng. J.*, **359**, 1550-1562 (2019)
 12. P. Gu, J. Xing, T. Wen, R. Zhang, J. Wang, G. Zhao, T. Hayat, Y. Ai, Z. Lin and X. Wang, Experimental and theoretical calculation investigation on efficient Pb(II) adsorption on etched Ti₃AlC₂ nanofibers and nanosheets. *Environ. Sci.: Nano*, **5**, 946-955 (2018)
 13. Y. Cai, L. Chen, S. Yang, L. Xu, H. Qin, Z. Liu, L. Chen, X. Wang, and S. Wang Rational Synthesis of Novel Phosphorylated Chitosan-Carboxymethyl Cellulose Composite for Highly Effective Decontamination of U(VI). *ACS Sustainable Chem. Eng.*, **7**, 5393-5403 (2019)
 14. L. Yin, Y. Hu, R. Ma, T. Wen, X. Wang, B. Hu, Z. Yu, T. Hayat, A. Alsaedi and X. Wang, Smart construction of mesoporous carbon templated hierarchical Mg-Al and Ni-Al layered double hydroxides for remarkably enhanced U(VI) management. *Chem. Eng.*, **359**, 1550-1562 (2019)
 15. J. Wang, Y. Shen, S. Liu and Y. Zhang, Single 2D MXene precursor-derived TiO₂ nanosheets with a uniform decoration of amorphous carbon for enhancing photocatalytic water splitting. *Appl. Catal. B.*, **270**, 118885-118861 (2020)
 16. P. Gu, S. Zhang, X. Li, X. Wang, T. Wen, R. Jehan, A. Alsaedi, T. Hayat and X. Wang, Recent advances in layered double hydroxide-based nanomaterials for the removal of radionuclides from aqueous solution. *Environ Pollut.*, **240**, 493-505 (2018)
 17. Y. Zou, Y. Liu, X. Wang, G. Sheng, S. Wang, Y. Ai, Y. Ji, Y. Liu, T. Hayat and X. Wang, Glycerol-Modified Binary Layered Double Hydroxide Nanocomposites for Uranium Immobilization via Extended X-ray Absorption Fine Structure Technique and Density Functional Theory Calculation. *ACS Sustainable Chem. Eng.*, **5**, 3583-3595 (2017)